Glycobiology, 2015, vol. 25, no. 7, 792–803
doi: 10.1093/glycob/cwv020
Advance Access Publication Date: 24 March 2015
Original Article

OXFORD

Original Article

Crystal structure of a *Xenopus laevis* skin prototype galectin, close to but distinct from galectin-1

Yasuhiro Nonaka[2], Takashi Ogawa[2], Hiromi Yoshida[3], Hiroki Shoji[2,4], Nozomu Nishi[3], Shigehiro Kamitori[3], and Takanori Nakamura[2,1]

[2]Department of Endocrinology, Faculty of Medicine, [3]Life Science Research Center, Kagawa University, Kagawa, Japan, and [4]Department of Biology, Kanazawa Medical University, Ishikawa, Japan

[1]To whom correspondence should be addressed: Tel: +81-87-891-2106; Fax: +81-87-891-2108; e-mail: tnaka@med.kagawa-u.ac.jp

Received 9 September 2014; Revised 9 March 2015; Accepted 22 March 2015

Abstract

Xenopus laevis (African clawed frog) has two types of proto-type galectins that are similar to mammalian galectin-1 in amino acid sequence. One type, comprising xgalectin-Ia and -Ib, is regarded as being equivalent to galectin-1, and the other type, comprising xgalectin-Va and -Vb, is expected to be a unique galectin subgroup. The latter is considerably abundant in frog skin; however, its biological function remains unclear. We determined the crystal structures of two proto-type galectins, xgalectin-Ib and -Va. The structures showed that both galectins formed a mammalian galectin-1-like homodimer, and furthermore, xgalectin-Va formed a homotetramer. This tetramer structure has not been reported for other galectins. Gel filtration and other experiments indicated that xgalectin-Va was in a dimer–tetramer equilibrium in solution, and lactose binding enhanced the tetramer formation. The residues involved in the dimer–dimer association were conserved in xgalectin-Va and -Vb, and one of the *Xenopus (Silurana) tropicalis* proto-type galectins, but not in xgalectin-Ia and -Ib, and other galectin-1-equivalent proteins. Xgalectin-Va preferred Galβ1-3GalNAc and not Galβ1-4GlcNAc, while xgalectin-Ib preferred Galβ1-4GlcNAc as well as human galectin-1. Xgalectin-Va/Vb would have diverged from the galectin-1 group with accompanying acquisition of the higher oligomer formation and altered ligand selectivity.

Key words: amphibian skin secretion, galectin, *Xenopus laevis*, X-ray crystallography

Introduction

Galectins, a β-galactoside-specific soluble lectin family, are widely distributed in metazoans and fungi (Barondes, Castronovo, et al. 1994; Barondes, Cooper, et al. 1994; Cooper and Barondes 1999; Cooper 2002). More than 15 members have been identified in mammals, and are classified into three structural types, such as proto, chimera and tandem-repeat types (Hirabayashi and Kasai 1993; Cooper 2002; Sato et al. 2009; Than et al. 2012). The galectin family members show a variety of expression patterns, ligand specificities and biological functions. Mammalian galectin-1, one of the most studied galectins, is a representative proto-type galectin, which comprises only a carbohydrate-binding domain. Galectin-1 is expressed in many tissues and cells, and is involved in many functions such as induction of cell death, cell adhesion and differentiation (Camby et al. 2006; Rabinovich et al. 2007).

The galectin family is interesting with regard to molecular evolution, because of its widely divergent functions and structures. Some mammalian galectins, including galectin-1, regulate a variety of immune cells (Rabinovich et al. 2007). Galectin-7 in keratinocytes is involved in wound healing (Cao et al. 2002). Congerin, a conger eel galectin, agglutinates certain kinds of bacteria (Kamiya et al. 1988; Nakamura et al. 2007). Recently, a marine sponge (*Cinachyrella* sp.) galectin was reported to modulate glutamate receptor ion channels (Ueda et al. 2013; Copits et al. 2014). These functions can be controlled through the mode of multivalency as well as the ligand-binding specificity (Brewer 2002; Earl et al. 2011). The homodimer of galectin-1 is a well-known galectin

© The Author 2015. Published by Oxford University Press. All rights reserved. For permissions, please e-mail: journals.permissions@oup.com

Downloaded from https://academic.oup.com/glycob/article/25/7/792/1988836 by guest on 16 August 2022

quaternary structure. Galectin-1 forms a dimer via the interface composed of the terminal β-strands to expand the two β-sheets. An oligomer of the chimera-type galectin is attained through the association with the non-carbohydrate-binding domain (Ahmad et al. 2004). In addition, several non-mammalian galectins have been reported to form oligomers in unique manners (Shirai et al. 1999; Walser et al. 2004; Ban et al. 2005; Freymann et al. 2012).

Secretions from amphibian skin have been studied as a source of antimicrobial substances, toxins and other bioactive molecules (Cardoso et al. 2014; Conlon et al. 2014). Skin galectins from *Xenopus laevis* were reported to be considerably abundant in granular glands of the skin (5% of the total proteins) (Marschal et al. 1994). When a frog faces stressful circumstances, the granular glands are caused to contract by catecholamine to excrete the compounds. Therefore, the skin galectins are expected to play a role in the defense against predators and/or infection. The two skin proto-type galectins from *X. laevis*, xgalectin-Va and -Vb, were identified in previous works (Marschal et al. 1992; Shoji et al. 2003). Two other proto-type galectins, xgalectin-Ia and -Ib, have also been identified (Shoji et al. 2002). While xgalectin-Va and -Vb are predominantly expressed in the skin, xgalectin-Ia and -Ib are expressed widely in the frog body like mammalian galectin-1. Both the DNA and amino acid sequences of human galectin-1 are more similar to those of xgalectin-Ia/Ib than to those of xgalectin-Va/Vb (Table I). From these observations, xgalectin-Ia and -Ib were assigned as equivalent proteins to mammalian galectin-1.

Xenopus laevis is an allotetraploid, which would be the reason for the existence of the two similar skin galectins and the two similar galectin-1-like proteins. The primary sequence identity of xgalectin-Va and -Vb is 78%, and that of xgalectin-Ia and -Ib is 91%. In this study, we chose xgalectin-Va for analysis, because xgalectin-Va is more abundant in the skin than xgalectin-Vb. The expression profiles of xgalectin-Ia and -Ib vary by tissue. For example, the major galectin in liver is -Ia, and that in kidneys is -Ib (Shoji et al. 2002, 2003). We analyzed xgalectin-Ib, because the recombinant protein could be obtained more efficiently than for xgalectin-Ia.

We determined the crystal structures of xgalectin-Va and -Ib. We revealed that xgalectin-Va formed a homotetramer through dimer–dimer association, while xgalectin-Ib only formed a dimer in the same manner as human galectin-1. Xgalectin-Va had a different carbohydrate specificity compared with xgalectin-Ib and human galectin-1. It was suggested that the frog skin galectins diverged from the galectin-1 group to perform a novel function with accompanying tetramer formation capability and altered ligand specificity.

Results

X-ray crystallographic structures of Xenopus galectins

The crystal structures of xgalectin-Va and -Ib are presented in Figure 1A and B. The two crystals belonged to the C2 space group (Table II). There were two protein molecules per asymmetric unit for xgalectin-Va, and one per unit for xgalectin-Ib. Both structures comprised a β-sandwich composed of six-stranded (S1–S6) and five-stranded (F1–F5) β-sheets, which is typical of the galectins so far reported. The root-mean-square deviation values for *Cα* atoms among human galectin-1, xgalectin-Ib and xgalectin-Va were comparable (Table I), although the amino acid sequence similarity of human galectin-1 and xgalectin-Ib was greater than those of the two other pairs.

The structures were obtained for the lactose-bound forms. Although lactose was not intentionally added to the xgalectin-Va sample, the electron density of carbohydrate was clearly observed at the ligand-binding site. The lactose used for the purification was not completely removed on dialysis. We also prepared a xgalectin-Va sample in the absence of lactose exclusively; however, in contrast to the lactose-containing sample, no fine crystal was obtained on screening. In the case of xgalectin-Ib, lactose was intentionally added to the sample during dialysis. Dynamic light scattering (DLS) measurements suggested that xgalectin-Va and -Ib were rather unstable in the absence of lactose.

The crystal structures indicated that the lactose-binding modes of these two galectins were basically consistent with those of the other reported galectins. However, Arg74 in human galectin-1, one of the seven key residues for the ligand binding, was replaced by Lys76 in xgalectin-Va. Lys76 in xgalectin-Va interacted with the glucose 2-OH group via a water molecule (Figure 1C), while Arg74 in xgalectin-Ib directly interacted with the glucose 2-OH group (Figure 1E). In addition to the key residues, Arg32, Tyr54 and Ser55 of xgalectin-Va, and His52 (indirect) and Glu53 of xgalectin-Ib were involved in the lactose binding (Figure 1D and F). In the binding cleft of xgalectin-Va, a malonate molecule, which was from the crystallization reservoir, was observed next to the lactose (Figure 1D). Elongation or modification of the non-reducing end of the ligand will fill this space.

An intramolecular disulfide bridge was observed between Cys17 and Cys89 of xgalectin-Ib. The electron density map showed both free and bonded cysteine residues (Supplementary data, Figure S1). Disulfide bonding of this cysteine pair in vitro was also reported for bovine galectin-1 (Cys16–Cys88) (Tracey et al. 1992; Bourne et al. 1994). These cysteines are conserved in many other galectin-1s, but are not conserved in xgalectin-Va/Vb. There were two vicinal pairs of cysteine residues (Cys46–Cys48 and Cys97–Cys112) in xgalectin-Va; however, there was no disulfide bond in the crystal structure.

The PDBePISA server (Krissinel and Henrick 2007) proposed a possible homodimer of xgalectin-Ib (Figure 2A) and a homotetramer of xgalectin-Va (Figure 2B). The dimer of xgalectin-Ib was consistent with those of galectin-1s from other vertebrates. Two intermolecular β-sheets were formed by the F1 and S1 strands. The homotetramer of xgalectin-Va also included a galectin-1-like homodimer (Mol-A and -B in Figure 2B). The tetramer was formed through the symmetric association of two dimers (Mol-A/B and -C/D). PDBePISA estimated that the

Table I. Comparison of DNA and amino acid sequences, and tertiary structures of three proto-type galectins

	Identity of DNA sequences (%)	Similarity of protein sequences (%)[a]	RMSD for Cα in crystal structures (Å)[b]
Human G1 versus xGIb[c]	57.5	68.9	0.80
Human G1 versus xGVa	50.6	53.3	0.75
xGVa versus xGIb	59.4	63.5	0.83

[a]Protein sequence similarity was calculated using the matrix BLOSUM62.

[b]Calculated for 129 Cα atoms, which excluded the gap sites and several terminal residues, was used for calculation. Structure of human galectin-1 is from PDB entry 1GZW.

[c]Human G1, human galectin-1; xGIb, xgalectin-Ib; xGVa, xgalectin-Va.

Downloaded from https://academic.oup.com/glycob/article/25/7/792/1988836 by guest on 16 August 2022

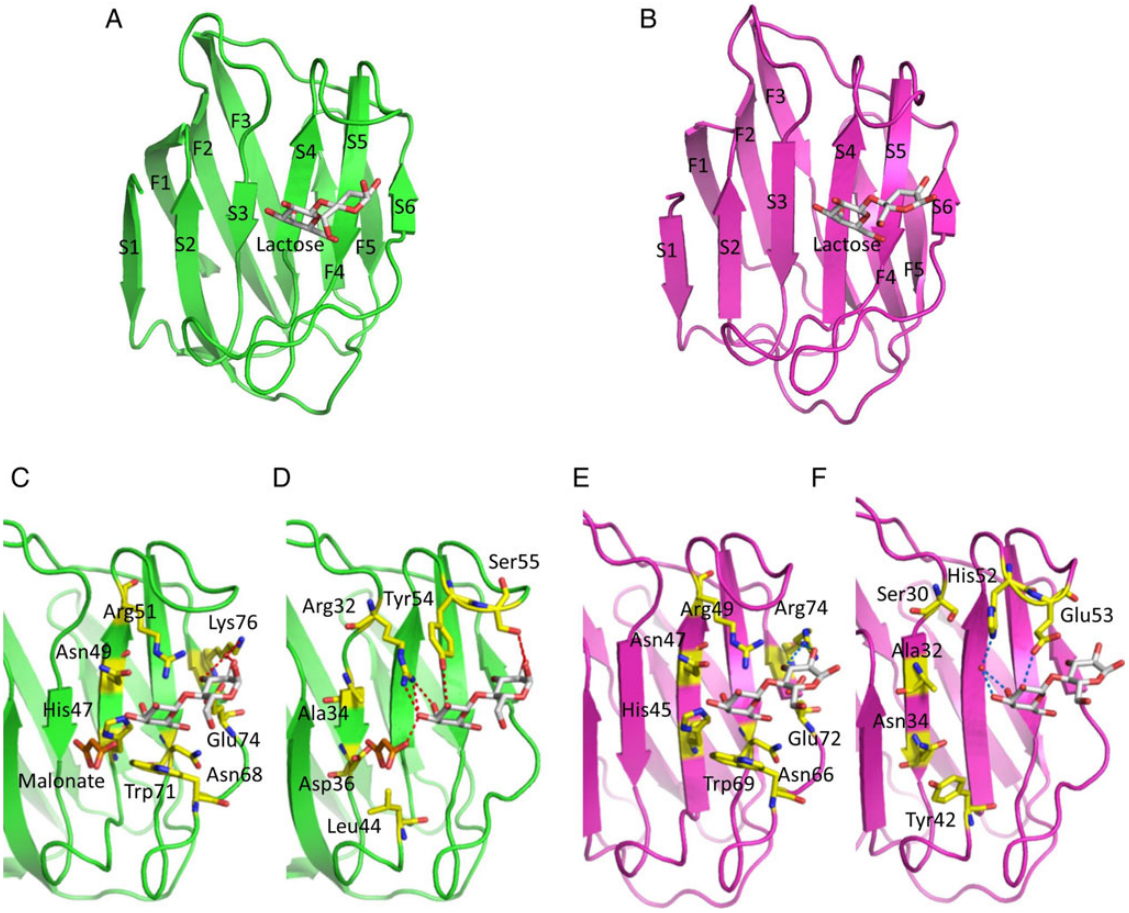

Fig. 1. Crystal structures of xgalectin-Va (**A**, **C**, **D**) and xgalectin-Ib (**B**, **E**, **F**) protomers. The cartoon models were generated using PyMol. The lactose and malonate molecules are shown as stick models. (**A**) Overall protomer structure of xgalectin-Va. (**B**) Overall protomer structure of xgalectin-Ib. (**C**) Lactose-binding site of xgalectin-Va. The seven residues that are the hallmarks of galectin are shown as sticks. Only the interaction of Lys76-lactose is shown. (**D**) Other residues encompassing the ligand-binding pocket of xgalectin-Va. (**E**) Lactose-binding site of xgalectin-Ib. The hallmark residues are shown as sticks. Only the interaction of Arg74-lactose is shown. (**F**) Other residues encompassing the ligand-binding pocket of xgalectin-Ib. This figure is available in black and white in print and in color at *Glycobiology* online.

interface area of Mol-A and -B was 580.6 Å^2, and that of Mol-A and -D was 464.7 Å^2. The interface of the dimer–dimer association mainly involved the F2 and F3 strands, and the S6–F3 and F4–F5 loops. For 10 residues, over 50% of the surface was buried by the Mol-A and -D interaction. These residues included five hydrophobic residues, Pro81, Met89, Ile91, Pro103 and Gly105 (Figure 2C). The hydrophobic interaction of these residues would contribute to this association. Furthermore, there were hydrogen bonds, Lys83N-Asp104O and Ser86Oγ-Gly105O, and salt bridges, Glu21Oε-Arg23Nη, between Mol-A and -D (Figure 2D).

Oligomer formation of xgalectin-Va and -Ib in solution

The oligomer formation of xgalectin-Va and -Ib was examined by DLS measurements (Figure 3). The hydrodynamic radius of xgalectin-Va at 32 μM with lactose was ~3.3–3.5 nm, corresponding to a 55–60 kDa globular protein. In the absence of lactose, the radius and estimated molecular weight were reduced, 3.0–3.2 nm and 45–50 kDa, respectively. These values were significantly larger than those for human galectin-1 (~2.7 nm, 35 kDa, data not shown). The results suggested that xgalectin-Va formed a higher oligomer than a dimer, and that the formation of this oligomer was promoted by lactose binding. The radius of xgalectin-Ib was 2.6–2.7 nm regardless of whether lactose was added or not, corresponding to ~30 kDa. These data were comparable with those for human galectin-1, suggesting galectin-1-like dimer formation.

Gel-filtration chromatography of xgalectin-Va also demonstrated the presence of a higher oligomer component (Figure 4). Xgalectin-Va gave two distinct elution peaks. Compared with the standard proteins, the former component was ~52 kDa, and the other one was ~34 kDa. Although the interaction between galectin and the Superdex gel could affect the elution pattern, at least, xgalectin-Va adopted two forms of different sizes. The elution of xgalectin-Ib gave one peak at ~36 kDa. From the results of the DLS measurement and X-ray crystallography together, we determined that xgalectin-Va formed both a dimer and a tetramer in solution, while xgalectin-Ib predominantly formed a dimer.

The hydrodynamic radius of xgalectin-Va in the presence of lactose was larger than that in the absence of lactose. To confirm the lactose dependence of the tetramer formation, a chemical cross-linking experiment was performed using bis(sulfosuccinimidyl) suberate (BS^3). BS^3 (arm length: 11.4 Å) can cross-link Mol-A and -D, as the distance between Lys83 and Lys106 is only 7.5–8.5 Å. Between Mol-A and -B, there are no Lys residues that can be cross-linked. In the experiment, a component of 30 kDa was detected concentration dependently (Figure 5). This would reflect association–dissociation

Downloaded from https://academic.oup.com/glycob/article/25/7/792/1988836 by guest on 16 August 2022

Table II. Data collection and refinement statistics

	Xgalectin-Va	Xgalectin-Ib
Data collection		
Space group	C2	C2
Unit cell parameters (Å)	$a = 102.65$, $b = 48.87$, $c = 61.09$	$a = 67.21$, $b = 35.32$, $c = 58.51$
	$\alpha = \gamma = 90°$, $\beta = 114.08°$	$\alpha = \gamma = 90°$, $\beta = 111.82°$
Resolution range (Å)	37.85–1.60 (1.66–1.60)	18.92–1.68 (1.74–1.68)
Total no. of reflections	128,845	56,478
No. of unique reflections	36,200	13,973
Redundancy	3.56 (3.47)	4.04 (4.04)
Completeness (%)	98.7 (96.9)	94.8 (91.4)
R^{a}_{merge}	0.056 (0.172)	0.046 (0.344)
Mean $I/\sigma(I)$	12.8 (2.5)	14.3 (2.9)
Refinement statistics		
Resolution range (Å)	37.85–1.60 (1.64–1.60)	18.92–1.68 (1.72–1.68)
No. of reflections	34,389	13,263
Completeness (%)	98.7	94.7
R-factor (%)	18.2 (36.1)	19.7 (34.1)
R_{free} (%)	21.7 (40.5)	25.3 (35.3)
RMSD from ideal values		
Bond length (Å)	0.023	0.019
Bond angles (°)	2.267	2.152
PDB ID code	3WUC	3WUD

[a] $R_{merge} = \sum_h \sum_i |I_{hi} - \langle I_h \rangle| / \sum_h \sum_i \langle I_h \rangle$.

of Mol-A and -D at micromolar concentrations. The small amount of the cross-linked component could be due to low efficiency of the cross-linking. Intramolecular Lys28 is also close to Lys83 (5.7–8.8 Å), and thus it will compete with the intermolecular cross-linking. At least, the cross-linking was clearly enhanced when lactose was present. This result was consistent with that of the DLS measurement. For xgalectin-Ib, the distance between the Lys128 residues of Mol-A and -B is 11.8 Å. A cross-linked component (~28 kDa) was detected after the BS^3 treatment of xgalectin-Ib, and lactose dependence was not observed (data not shown).

Lectin activities of xgalectin-Va and -Ib

The hemagglutination activities of xgalectin-Va and -Ib were examined using trypsin-treated rabbit erythrocytes (Supplementary data, Figure S2). In spite of the higher oligomer formation, xgalectin-Va exhibited much lower activity (400–800 nM) than xgalectin-Ib (6.25–12.5 nM) and human galectin-1 (3.13–6.25 nM). The activity of the galectin purified from *X. laevis* skin secretion was estimated to be comparable with that of recombinant xgalectin-Va. The binding affinity of xgalectin-Va as to the saccharides on the red blood cell surface would be weak.

Carbohydrate-binding affinities were compared among the three galectins by fluorescence spectroscopy and surface plasmon resonance measurement. We compared three basic galectin-binding disaccharides, lactose (Galβ1–4Glc), *N*-acetyllactosamine (LacNAc, Galβ1–4GlcNAc) and core-1 with a threonine residue (Galβ1–3GalNAcαThr). The fluorescence spectra of the galectins were blue-shifted and quenched upon carbohydrate binding (Supplementary data, Figure S3). The dissociation constants (K_d) estimated on Hill plot analyses are shown in Table III. The values for human galectin-1 were comparable with those estimated by other methods (Nesmelova et al. 2010; Iwaki et al. 2011). Human galectin-1 and xgalectin-Ib preferred LacNAc to lactose, and hardly bound to core-1. On the other hand, xgalectin-Va strongly bound to lactose and core-1, but the affinity to LacNAc was relatively weak.

A surface plasmon experiment involving a sensor chip with asialofetuin immobilized on it was performed to measure the inhibitory effects of the saccharides on galectin-asialofetuin binding (Supplementary data, Figure S4). The IC_{50} values are also informative for comparing the binding specificities. The results were qualitatively consistent to those obtained on fluorescence spectroscopy (Table III). When the protein concentration is much smaller than K_d, IC_{50} is theoretically approximate to K_d for monovalent binding, and IC_{50} can deviate from K_d for multivalent binding. The obtained values for xgalectin-Va were larger than expected from the results of fluorescence spectroscopy maybe reflecting the higher oligomer formation.

Amino acid sequence analyses

We searched the NCBI Reference Sequence database for the galectin sequences of diploid clawed frog *Xenopus (Silurana) tropicalis*. We obtained these two sequences: "uncharacterized protein LOC100216286" (accession ID, NP_001135709), which is quite similar to xgalectin-Va and -Vb, and "predicted galectin-1-like" (XP_002934260), which is quite similar to xgalectin-Ia and -Ib. In this study, we name these proteins xtgalectin-V and -I, respectively. Galectin-1 orthologs have also been reported for other frogs, *Rhinella (Bufo) arenarum* (Argentine toad) and *Rana catesbeiana* (bullfrog) (Ahmed et al. 1996; Uchiyama et al. 1997). However, these galectins are present particularly in ovary. The skin gland galectins may be a hallmark of the Xenopodinae, and may be related to their behavior, i.e., exclusively aquatic.

We estimated the evolutionary distances from the amino acid sequences of representative proto-type galectins. The mean distance among xgalectin-Va, -Vb and xtgalectin-V was 0.239 ± 0.013; among xgalectin-Ia, -Ib and xtgalectin-I was 0.108 ± 0.009; and between the two groups was 1.065 ± 0.054, suggesting that these two groups are distinct. We grouped the former three galectins as "xgalectin-V", and the latter three as "xgalectin-I", respectively. The distances showed that these groups, especially xgalectin-I, were closer to mammal and chicken galectin-1 than to galectin-2, and fish galectin-1 (data not shown).

Downloaded from https://academic.oup.com/glycob/article/25/7/792/1988836 by guest on 16 August 2022

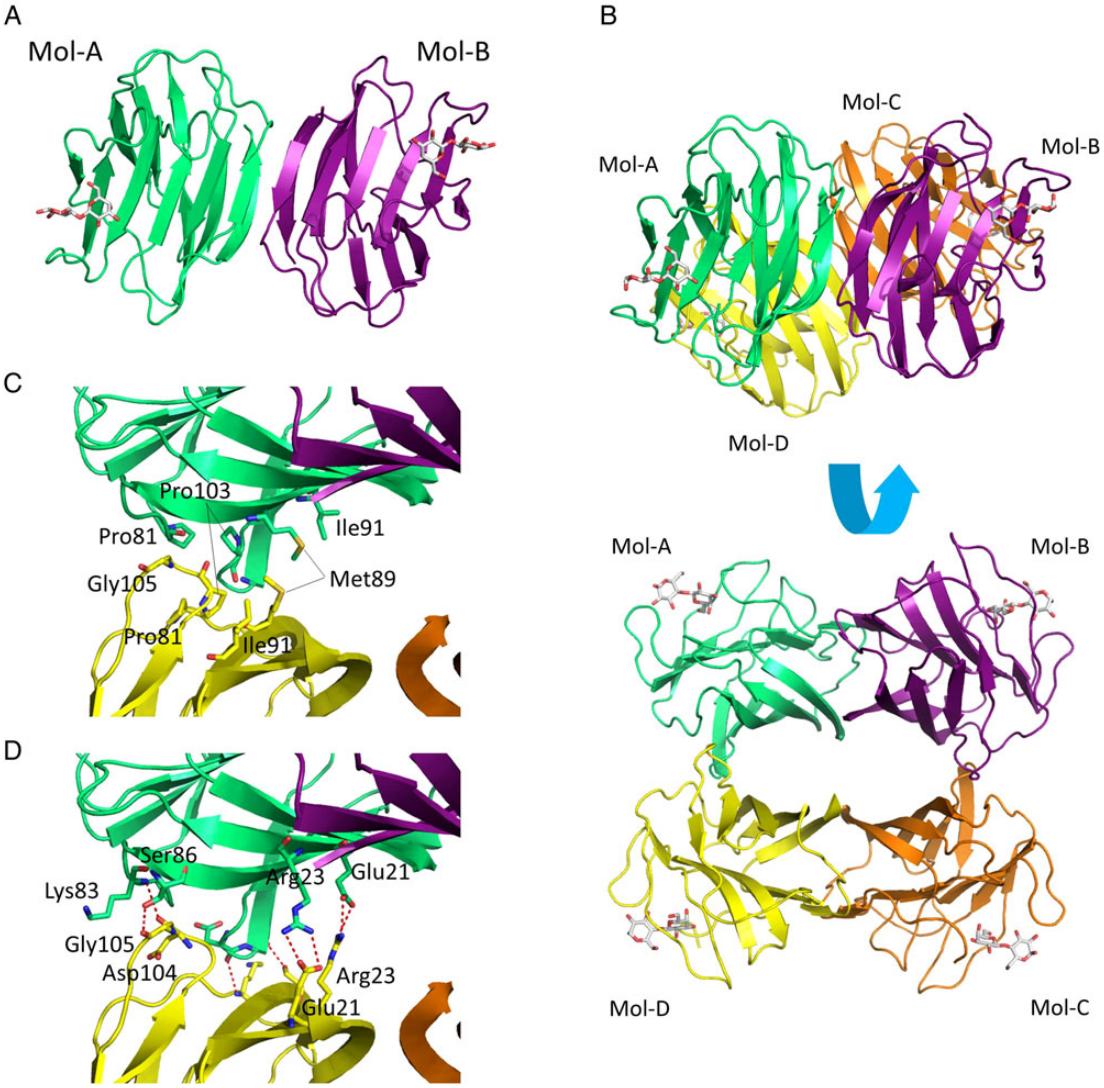

Fig. 2. (**A**) Dimer structure of xgalectin-Ib proposed by PDBePISA. An asymmetric unit is composed of one protein molecule, Mol-A. Mol-B was generated by symmetry operation (*–x, y* and *–z*) of Mol-A. (**B**) Tetramer structure of xgalectin-Va proposed by PDBePISA. An asymmetric unit is composed of Mol-A and -B. Mol-C and -D were generated by symmetry operation (*–x, y* and *–z*) of Mol-A and -B. (**C**) Hydrophobic residues buried by the association of Mol-A and -D. (**D**) Salt bridges and hydrogen bonds formed between Mol-A and -D. This figure is available in black and white in print and in color at *Glycobiology* online.

We reconstructed a phylogenetic tree from the amino acid sequences using the maximum likelihood method (Figure 6). The three xgalectin-V proteins clustered together with a large bootstrap value, and so did the xgalectin-I proteins. These two groups were close to each other, and they should probably be included in the tetrapod galectin-1 group. The previous comprehensive phylogenetic analysis also revealed that xgalectin-Ia, Ib, Va (denoted as Ic in that article) and Vb were included in the tetrapod galectin-1 group on the tree obtained by the distance method (Houzelstein et al. 2004).

Discussion

The crystallography and other experiments indicated the tetramer formation of xgalectin-Va. The tetramer was detected with micromolar concentrations (Figures 3, 4 and 5), however, it seemed to easily dissociate upon dilution, as suggested by the observation that the gel-filtration conditions (such as the sample volume) significantly affected the dimer–tetramer ratio (data not shown). Does this weak

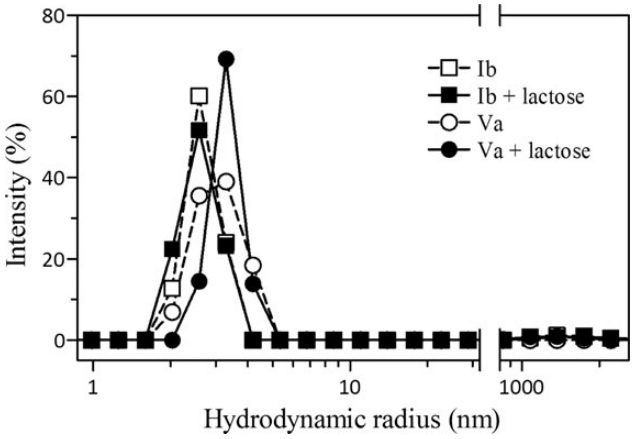

Fig. 3. Representative DLS data for xgalectin-Ib (square) and -Va (round), in the absence (open symbols) and presence (closed symbols) of lactose. The intensity of the scattering components was plotted.

Downloaded from https://academic.oup.com/glycob/article/25/7/792/1988836 by guest on 16 August 2022

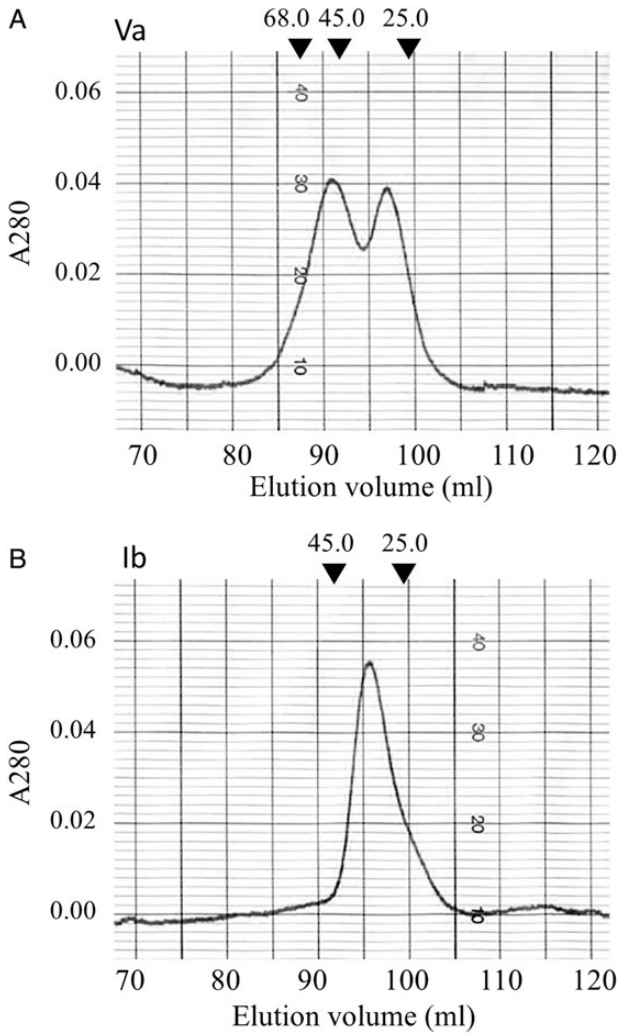

Fig. 4. Gel-filtration chromatography of xgalectin-Va (top) and -Ib (bottom). Triangles indicate the elution volumes of marker proteins (25.0 kDa, chymotrypsinogen A; 45.0 kDa, ovalbumin; 68.0 kDa, bovine serum albumin).

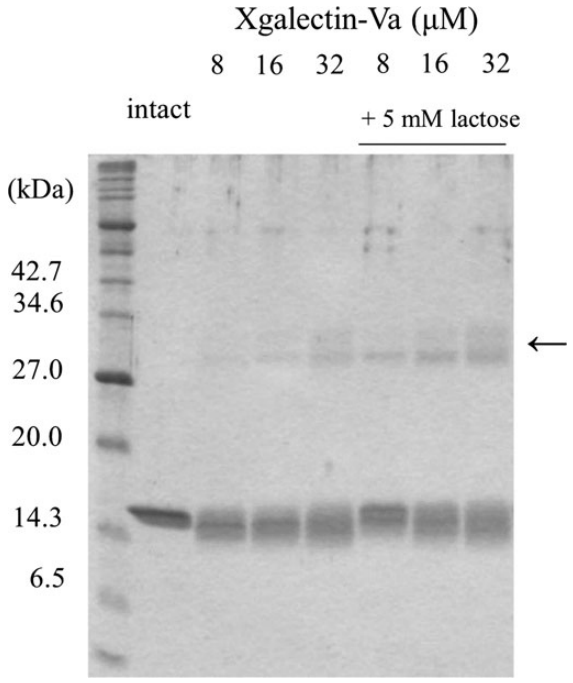

Fig. 5. Chemical cross-linking of xgalectin-Va. The intact sample was not incubated with BS^3. The other samples were incubated with BS^3, and diluted to the same concentration. The arrow indicates the cross-linked component.

Table III. Affinities of three proto-type galectins to carbohydrates

	Lactose	LacNAc	Core-1-Thr
Xgalectin-Va			
K_d[a]	7.1	660	3.3
IC_{50}[b]	39 μM	1700 μM	23 μM
Xgalectin-Ib			
K_d	180	41	–[c]
IC_{50}	150 μM	49 μM	>3200 μM
Human galectin-1			
K_d	140	44	–
IC_{50}	170 μM	39 μM	>3200 μM

[a]Dissociation constant (K_d) estimated by fluorescent spectroscopy.

[b]Half-inhibition concentration (IC_{50}) estimated by surface plasmon resonance measurement with an asialofetuin-immobilized sensor chip.

[c]Not determined. The binding was slightly detected with 1 mM carbohydrate.

oligomerization have any biological significance? When we obtained ~1 mL of secretion from frog skin by adrenalin stimulation, the galectin purified from this secretion by affinity chromatography amounting to ~1.5 mg. The skin galectins would be stored at much higher than 1 mg/mL (>60 μM) in skin glands, and therefore the tetramer can be formed in glands and just after secretion. It is possible that the high concentration storage of galectin in glands is facilitated by the tetramer formation, which reduces the accessible molecular surface to prevent non-specific aggregation.

If a lectin-glycan lattice or aggregation is firmly constructed with natural ligands, the tetramer can be maintained even when diluted. Homogeneous lattice structures will stabilize the intermolecular contacts. Weak oligomerization is also observed for other lectins, and the lectin–carbohydrate lattice formation depends on such weak interactions (Hamelryck et al. 2000). Furthermore, clustering of lectins through multivalent ligands is also considered to enhance lectin aggregation. The hemagglutination by human galectin-1 observed at nanomolar concentrations (Supplementary data, Figure S2) could be due to these effects. Human galectin-1 exists mainly as monomers at these concentrations, according to the low-micromolar dimer dissociation constant (Salomonsson et al. 2010).

The mechanism of the tetramer enhancement on lactose binding (Figures 3 and 5) is unclear at present. X-ray crystallography of other galectins revealed that carbohydrate binding to most galectins did not induce major changes in the overall structure. On the other hand, the recent studies on galectin-1, -3 and -7 involving NMR and MD simulation revealed changes in structural dynamics not only at the ligand binding site but also at distant sites (Diehl et al. 2010; Nesmelova et al. 2010; Ermakova et al. 2013). The human galectin-7 dimer, of which the interface is opposite to the ligand binding site, is stabilized by lactose binding (Leonidas et al. 1998; Ermakova et al. 2013). Motional changes, rather than minor static changes, are considered to be a major factor for this dimer stabilization. Like galectin-7, the xgalectin-Va tetramer could also be stabilized through a long-range effect on the structural dynamics.

Downloaded from https://academic.oup.com/glycob/article/25/7/792/1988836 by guest on 16 August 2022

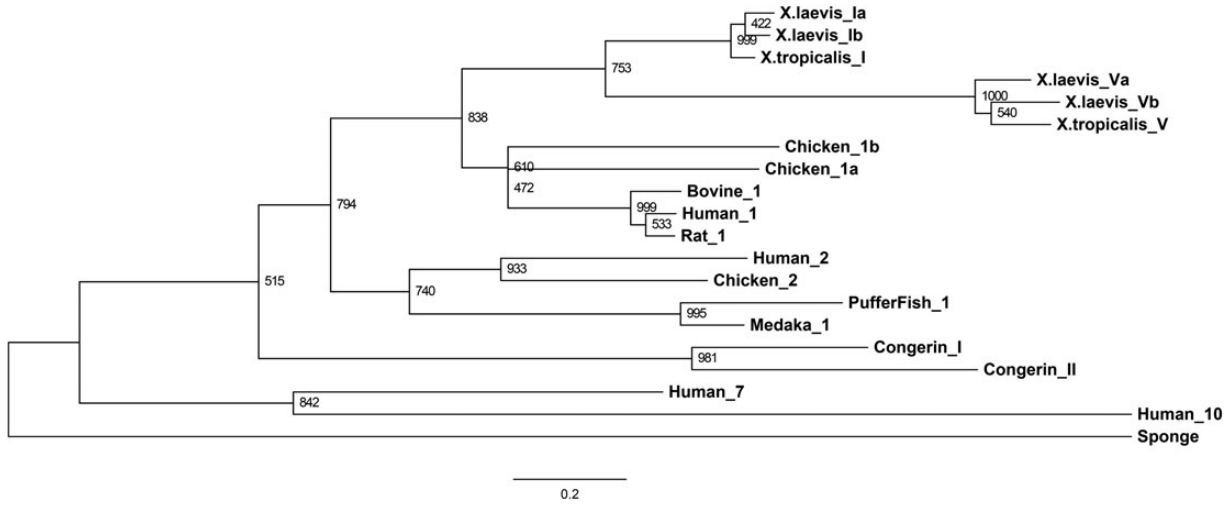

Fig. 6. Phylogenetic tree of representative proto-type galectins based on the amino acid sequences. To construct the tree, alignment was performed using ClustalW. The tree was constructed using the maximum likelihood method in the package of MEGA6 with the WAG+G+I model. The bootstrap values were calculated using 1000 replicates. The root was placed on the marine sponge galectin branch. NCBI accession ID: xgalectin-Va, NP_001079245; xgalectin-Vb, NP_001079042; xtgalectin-V, NP_001135709; xgalectin-Ia, NP_001079039; xgalectin-Ib, NP_001079744; xtgalectin-I, XP_002934260; human galectin-1, NP_002296; human galectin-2, NP_006489; human galectin-7, NP_002298; human galectin-10 NP_001819, NP_002296; bovine galectin-1, NP_786976; rat galectin-1, NP_063969; puffer fish galectin-1, XP_003979112; medaka galectin-1, XP_004071838; congerin-I, BAA36385; congerin-II, BAA36386; chicken galectin-1a, AAS59560; chicken galectin-1b, NP_990826; chicken galectin-2, XP_001234400; and marine sponge (*Cinachyrella* sp.) galectin, BAM09153.

Recently, as judged on crystallography, a marine sponge (*Cinachyrella* sp.) galectin was reported to form a homotetramer (Freymann et al. 2012), which is similar to but different from the xgalectin-Va tetramer (Figure 7A). The overall β-sandwich structure of the sponge galectin is twisted, and thus the tetramer is donut-shaped. When Mol-A of the sponge galectin was superposed on that of xgalectin-Va, their Mol-Bs greatly disagreed (Figure 7B). On the other hand, the backbone conformation of xgalectin-Va agreed well with those of xgalectin-Ib and human galectin-1 (Figure 7B and Table I). The difference in the surface residues between xgalectin-Va and -Ib would primarily contribute to the dimer–dimer association.

The primary sequences of the six clawed frog galectins and human galectin-1 were aligned by comparing the crystal structures (Figure 8). The residues involved in the tetramer formation were conserved in the three xgalectin-V proteins, and not necessarily conserved in the three xgalectin-I proteins (Figure 8, black). The hydrophobic residues at the dimer–dimer interface, Met89, Ile91 and Pro103, in xgalectin-Va are replaced by Ser87, Cys89 and Ser102 in xgalectin-Ib, respectively. Furthermore, Arg23 in the xgalectin-V group is replaced by Lys in the xgalectin-I group. Although a salt bridge can be formed by Lys, the greater distance between Lys and Glu will weaken this interaction. Ser86 in xgalectin-Va, of which the sidechain OH interacted with Gly105O, is replaced by Ala84 in xgalectin-Ib. The tetramer formation is considered to be a common property of the xgalectin-V group, while the xgalectin-I group proteins would predominantly form the dimer. This finding also supports the possibility that the tetramer is associated with the biological role of xgalectin-V.

In spite of the high affinity for lactose and the higher oligomer formation, the hemagglutination activity of xgalectin-Va was much weaker than those of xgalectin-Ib and human galectin-1 (Supplementary data, Figure S2). This may be due to its lower affinity for LacNAc (Table III). On the other hand, xgalectin-Va preferred the core-1 structure, which is one of the typical moieties of mucin. Enhancement of aggregation of the mucin from frog skin is one of the possible roles of the xgalectin-V proteins. If xgalectin-V also binds to microorganisms like congerins (Kamiya et al. 1988; Nakamura et al. 2007), it may induce aggregation of pathogens with secreted mucin. The higher oligomer formation will be beneficial for enhancing such aggregation. More detailed analyses are needed to clarify the biological function.

The high affinity of xgalectin-Va for lactose could be supported by Arg32, Tyr54 and Ser55 (Figure 1D), which are absent in xgalectin-Ib and human galectin-1. The selectivity for LacNAc and core-1 can be explained by the conformation of the S4–S5 loop. The backbone structures of the S4–S5 loops in xgalectin-Ib and human galectin-1 agree well, while that in xgalectin-Va is shifted toward the S6 strand (Figure 9A). This may be attributed to Val56 and Lys76 of xgalectin-Va (Gly54 and Arg74 of xgalectin-Ib and human galectin-1) (Figure 9B). The torsion angles of Gly54 in xgalectin-Ib (phi = 74.8° and psi = 5.1°) are not favored by a valine residue, thus xgalectin-Va cannot adopt such a conformation at this site. Furthermore, the salt bridge formed by Lys76 and Asp57 in xgalectin-Va (Arg74 and Asp55 in xgalectin-Ib) would affect the loop conformation, because a lysine residue is shorter than an arginine one.

We manually superimposed LacNAc and core-1 molecules onto the crystal structures, based on other galectin/carbohydrate complex structures (Figure 9B and C). The *N*-acetyl group of LacNAc approached Val56 of xgalectin-Va, suggesting conformational restriction of the *N*-acetyl group. On the other hand, for xgalectin-Ib and human galectin-1, Gly54 provides a space for the *N*-acetyl group. In the case of core-1, the *N*-acetyl group conflicts with Glu53 in xgalectin-Ib (His53 in galectin-1), while there is a space at this position in xgalectin-Va. This space is provided by the shift of the S4–S5 loop (Figure 9A) and the small Ser55 sidechain. Perhaps the loop structure of xgalectin-Va should be modulated to avoid LacNAc, which is abundant on animal organs, and to prefer specific glycan structures such as Galβ1–3GalNAc, which is typical of *O*-glycans. This carbohydrate selectivity is shared by xgalectin-Vb and xtgalectin-V, as suggested by the amino acid sequences (Figure 8).

Downloaded from https://academic.oup.com/glycob/article/25/7/792/1988836 by guest on 16 August 2022

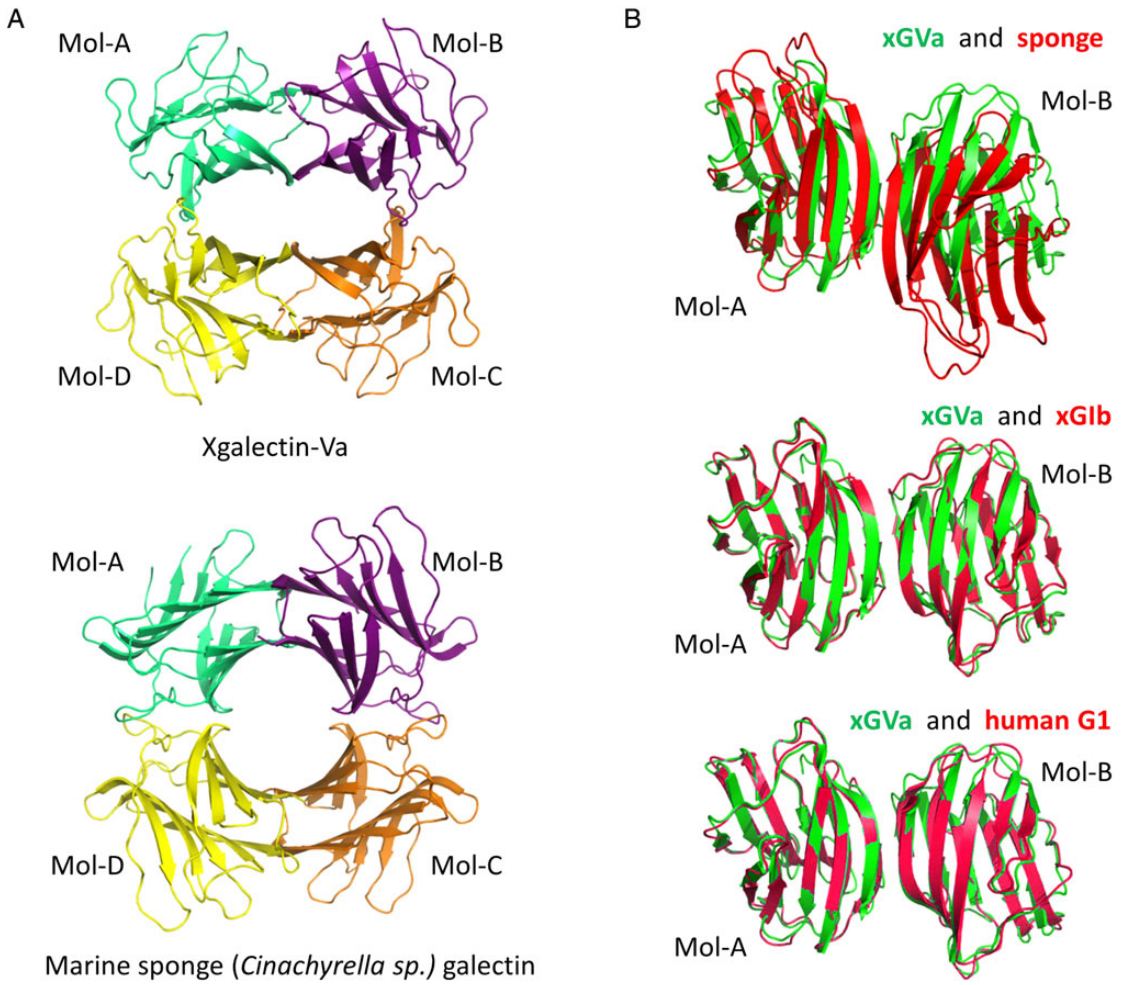

Fig. 7. Comparison of the structures of xgalectin-Va, xgalectin-Ib, human galectin-1 and a marine sponge galectin. The models were generated using PyMol. (**A**) Tetramer structures of xgalectin-Va and a marine sponge (*Cinachyrella sp.*) galectin (PDB ID: 4AGR). (**B**) Superimposition of marine sponge galectin, xgalectin-Ib (xGIb), and human galectin-1 (human G1, PDB ID: 1GZW) on xgalectin-Va (xGVa). The Mol-As were used for the fitting calculation by PyMol. This figure is available in black and white in print and in color at *Glycobiology* online.

```
                      10        20        30        40        50        60        70
Xgalectin-Va  MDMEPDVRIT NLNLHKGHRV EVRGRIAKGT NRFAVDLGTD SRNLICHCNP RFEYSVDKNT IVLNSKQNDV
Xgalectin-Vb  MDMQPDVKIT NLNLHKGHRV EVRGHISKDS SRFAVDLGTD CNNLICHCNP RFEFSEDKNT IIFNSKENDV
Xtgalectin-V  MAMQPDVTIT NLSLHKGHRV EVRGRILKDT KRFAVDMGAD AENLIMHCNP RFEFSVDKNT IIFNSKQNGV
Xgalectin-Ia  --MSAGMVMS NFSLKQGHCL ELKGIIPKDA KSFAINLGKD SSNYVIHFNP RFDHHGDTNK IICNSKEENH
Xgalectin-Ib  --MAAGMVMN NFSLKQGHCL ELKGFIPKDA KSFAINLGKD SSNYVIHFNP RFDHEGDTNK IICNSKEENS
Xtgalectin-I  --MAAGIVMN NFSLKQGHCL ELKGLIPKDA KSFAINLGKD SSNYVLHFNP RFDHQGDNKK IICNSKEENC
Human G1      --MACGLVAS NLNLKPGECL RVRGEVAPDA KSFVLNLGKD SNNLCLHFNP RFNAHGDANT IVCNSKDGGA
                                                        * *  *  ###  *

                      80        90        100       110       120       130
Xgalectin-Va  WDIEKKETAF EFKSGSETML IFDFE-DCIT VHLPDGKEIP FTCRFPIEVI NYLALN-NIE LISISVH
Xgalectin-Vb  WGTEQKEVAF EFKAGSQTML IFEFG-DCIN VHLPDGTDIP FACRFPIQVI NYLALY-NLQ LISISVH
Xtgalectin-V  WGTEQKETAF EFQAGSETML IFEFE-DCIT VLLPDGTEVP FTCRFPIDVI NYLALY-NLE LISISVH
Xgalectin-Ia  WGKEQRENAF EFQQGAETTI CFEYQADHLK VKLSDGKEFN FPIRMPLDTI TFLTMD-GIE LKSFSLH
Xgalectin-Ib  WGTEQRENVF EFQQGAETSI CFEYQADHLK VKLSDGQEFN FPIRMPLDTI TFLSMD-GIE LKAISLH
Xtgalectin-I  WGKEQRETAF EFQQGAETSI CFEYQADHLK VKLSDGQEFT FPIRMPLDTI TFLCMD-GIE LKSFSLH
Human G1      WGTEQREAVF EFQPGSVAEV CITFDQANLT VKLPDGYEFK FPNRLNLEAI NYMAADGDFK IKCVAFD
              *  * *
```

Fig. 8. Multiple alignment of six Xenopodinae proto-type galectins and human galectin-1. The alignment was performed by visually checking the crystal structures of xgalectin-Va, -Ib and human galectin-1. The xgalectin-Va/Vb-like and xgalectin-Ia/Ib-like proteins from *Xenopus (Silurana) tropicalis* are designated as xtgalectin-V and xtgalectin-I, respectively. Residues involved in the association of Mol-A and -D are highlighted in black. The seven consensus residues of the galectin family are indicated by asterisks. Residues in the S4–S5 loop involved in the ligand binding are indicated by sharps (#).

Downloaded from https://academic.oup.com/glycob/article/25/7/792/1988836 by guest on 16 August 2022

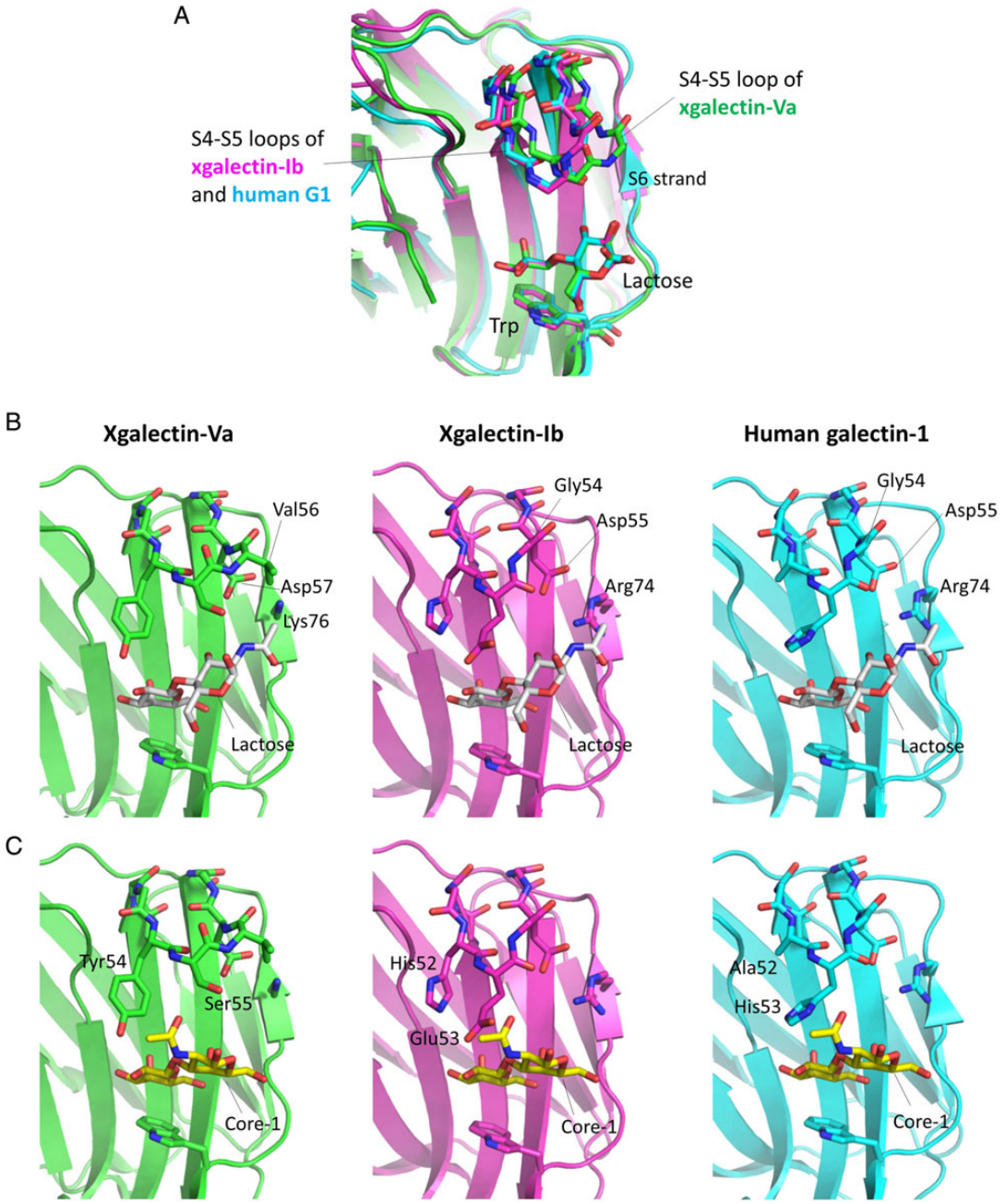

Fig. 9. (**A**) Superimposition of the crystal structures of xgalectin-Va, xgalectin-Ib, and human galectin-1 by fitting the lactose molecules. For the S4-S5 loops, only backbone atoms are shown as stick models. (**B** and **C**) Superimposition of carbohydrate molecules on the crystal structures. LacNAc (Galβ1-4GlcNAc, B) and core-1 (Galβ1-3GalNAc, C) were manually placed on the structures of xgalectin-Va, -Ib, and human galectin-1, according to the crystal structures of human galectin-1/LacNAc complex (PDB entry 1W6P) and human galectin-9 NCRD/GalNAcα1-3GalNAcβ1-3Gal complex (PDB entry 2EAL). This figure is available in black and white in print and in color at *Glycobiology* online.

The *X. laevis* galectin family was comprehensively characterized in the previous work (Shoji et al. 2003). Despite the sequence similarity to galectin-1, its abundant expression in skin glands and the presence of more galectin-1-like proteins suggested that xgalectin-Va/Vb should have a distinct function. In this study, xgalectin-Va showed different carbohydrate specificity and oligomer formation capability from xgalectin-Ib and human galectin-1, supporting that the xgalectin-V proteins can be regarded as a distinct subgroup from xgalectin-I. Secretory lectins may be valuable for aquatic life, such as for aggregation of mucin and/or microorganisms. Further comparative study will shed light on the functional and structural diversity of galectins.

Materials and methods

Preparation of protein samples

The cDNA sequences of the Xenopus galectins were determined in our previous work (Shoji et al. 2003). For the preparation of xgalectin-Va (NCBI accession ID, NP_001079245) and -Ib (ID, NP_001079744), the cDNAs were incorporated into the pGEX4T-2 vector using

Downloaded from https://academic.oup.com/glycob/article/25/7/792/1988836 by guest on 16 August 2022

BamHI and XhoI, and also into the pET11a vector using NdeI and BamHI. Recombinant proteins were expressed in *E. coli* BL21 or BL21(DE3) cells. For the GST-fused proteins, the *E. coli* BL21 lysate was loaded onto a glutathione-Sepharose 4B (GE Healthcare, Waukesha, WI), and the column was washed with TBS. Then, the GST tag was removed with thrombin (Calbiochem, Darmstadt, Germany) on the column overnight at room temperature. The cleaved proteins were eluted from the column, and purified on a lactose-agarose column (Seikagaku, Tokyo, Japan). For the other proteins, the lysate was loaded onto a lactose-agarose column to purify the sample. The recombinant human galectin-1 Cys to Ser mutant (CS3) was also prepared using the *E. coli* expression system (pET11a vector, BL21(DE3) strain) as described previously (Nishi et al. 2008).

Natural skin galectins were collected from a piece of skin from a *X. laevis* that was knocked out in ice water. The skin was soaked in an adrenaline solution (1 mg/mL adrenaline, 20 mM Tris–HCl, pH 7.5, 0.15 M NaCl) and then incubated for 20 min at room temperature. The skin was removed and the secretion was centrifuged at 2000 rpm for 5 min. The supernatant was additionally centrifuged at 15,000 rpm for 10 min, and then loaded onto a lactose-agarose column to purify the protein.

Crystallization and data collection

Protein samples for crystallography were prepared with 20 mM Tris–HCl (pH 7.2), 50 mM NaCl, 10 mM lactose (only for xgalectin-Ib), and 1–2 mM DTT. First, xgalectin-Va and -Ib were subjected to the initial screening using Crystal Screen I and II, PEG/ION Screen I and II, Index, SaltRx, Grid Screen Sodium Malonate (Hampton, CA), Wizard I and II (Emerald BioSystems, Washington) and PGA screen (Molecular Dimensions, Suffolk, UK) kits. Large single crystals of xgalectin-Va were obtained with a reservoir solution containing 2.4 M sodium malonate (pH 5.0) by the sitting drop method at 293 K. Single crystals of xgalectin-Ib were obtained with a reservoir solution containing 0.1 M MES (pH 6.0), 0.2 M ammonium sulfate and 34% polyethylene glycol 3350.

Data were collected with an R-AXIS VII system on a Rigaku MicroMax007HF rotating anode (CuKα) X-ray generator with VariMax optics (40 kV, 30 mA) (Rigaku, Tokyo, Japan) at a wavelength of 1.5418 Å and 100 K. A crystal of xgalectin-Ib was soaked in a solution containing 30% (v/v) ethylene glycol. All data were processed with the HKL2000 system (Otwinowski and Minor 1997) and the Crystalclear system (Rigaku).

Structure determination and refinement

The structures were solved by the molecular replacement method, using the program MOLREP (Vagin and Teplyakov 2000) packaged in CCP4 (Collaborative Computational Project, Number 4 1994). The search models used for xgalectin-Va and -Ib were the crystal structures of human galectin-1 (PDB: 1GZW) and xgalectin-Va, respectively. The program REFMAC5 (Murshudov et al. 1997) was used for the structure refinement, and COOT (Emsley and Cowtan 2004) was used for the model building. The atomic coordinates and structure factors have been deposited in the Protein Data Bank under accession codes 3WUC (xgalectin-Va) and 3WUD (xgalectin-Ib).

Dynamic light scattering

DLS measurements were carried out using a DynaPro Nanostar and DYNAMICS software (Wyatt Technology, Santa Barbara, CA). The acquisition time was 10 s and the number of acquisitions was 10–15. The acquisitions that showed inadequate baselines were omitted. All measurements were carried out at 293 K. The protein concentration was adjusted to 32 μM with 20 mM Tris–HCl (pH 7.2), 50 mM NaCl and 0 or 5 mM lactose.

Gel-filtration chromatography

Gel-filtration chromatography was performed using a Superdex 200 pg 16/60 column (GE Healthcare) equilibrated with 20 mM Tris–HCl, 250 mM NaCl, pH 7.2, 10 mM lactose, 0.01% sodium azide at 298 K. A protein solution with a concentration of 32 μM was loaded into a 200-μL sample loop. The flow rate was 0.5 mL/min, and the eluent was monitored at 280 nm. Chymotrypsinogen A (25 kDa), hen ovalbumin (45 kDa) and bovine serum albumin (68 kDa) were used as the molecular markers.

Chemical cross-linking experiment

Protein samples were incubated with a 25-fold molar excess of BS^3 (Dojindo Laboratories, Kumamoto, Japan) for 30 min at 298 K. The reaction solution contained 8 mM sodium phosphate, 5 mM HEPES and 85 mM NaCl (pH 7.5). The reaction was stopped by adding Tris–HCl buffer (pH 8.0) to the final concentration of 40 mM Tris–HCl. Then aliquots of the samples were mixed with SDS–PAGE loading buffer. The amount of the protein loaded on the SDS–PAGE gel was the same for each sample.

Hemagglutination assay

The hemagglutination assay was performed by the method previously described (Nowak et al. 1976). Samples were prepared by serial 2-fold dilution in a 96-well microtiter plate, being mixed with 0.1% bovine serum albumin (BSA) and 0.2 mM DTT in phosphate-buffered saline. Glutaraldehyde-fixed trypsin-treated rabbit erythrocytes with 0.1% BSA were added to each well to a final concentration of 2% (v/v). The plate was incubated for 1 h at room temperature. The minimum concentration required for hemagglutination was visually determined.

Fluorescence spectroscopy

Fluorescence spectra were measured using a JASCO FP-6300 (Jasco, Tokyo, Japan). The temperature of the cell holder was kept at 293 K. The excitation wavelength was 280 nm. The fluorescence intensity changes in the range of 320–400 nm were used to obtain a Hill plot. Assuming that each spectrum was composed of two spectra (unbound and bound), the least-square method was used to estimate each unbound–bound ratio (Supplementary data, Figure S3B). The protein concentration was adjusted to 16 or 32 μM with 10 mM sodium phosphate (pH 7.0), 50 mM NaCl and 1 mM DTT.

Surface plasmon resonance

Surface plasmon resonance experiments were performed using a BIAcore 2000 instrument (GE Healthcare). Asialofetuin was immobilized on a CM5 sensor chip. Various concentrations of a carbohydrate solution were mixed with 2 μM (xgalectin-Va) or 4 μM (human galectin-1 and xgalectin-Ib) protein in sodium phosphate buffer, pH 7.0, with 0.1 M NaCl, 2 mM DTT and 0.005% P20, and then incubated at room temperature for more than 20 min before measurements. Each sample was loaded at a flow rate of 10 μL/min for 4 min at 298 K.

Downloaded from https://academic.oup.com/glycob/article/25/7/792/1988836 by guest on 16 August 2022

Sequence alignment and phylogenetic analysis

The amino acid sequences of galectins were retrieved from the NCBI RefSeq database (www.ncbi.nlm.nih.gov/protein/, last accessed April 2, 2015). NCBI accession ID: xgalectin-Va, NP_001079245; xgalectin-Vb, NP_001079042; xtgalectin-V, NP_001135709; xgalectin-Ia, NP_001079039; xgalectin-Ib, NP_001079744; xtgalectin-I, XP_002934260; and human galectin-1, NP_002296. The ID numbers of the galectins used for the phylogenetic analysis are listed in Figure 6. The amino acid alignment in Figure 8 was performed by checking the superimposition of the crystal structures of xgalectin-Va, -Ib and human galectin-1 (PDB entry 1GZW).

The alignment for the phylogenetic tree construction was performed with ClustalW (clustalw.ddbj.nig.ac.jp/, last accessed April 2, 2015; gap opening penalty 10, gap extension penalty 0.05 and Gonet protein weight matrix). The tree was constructed using the maximum likelihood method in the software MEGA6 (Tamura et al. 2013) with the WAG (Whelan and Goldman 2001) + gamma ($\alpha = 2.31$) + invariant (1.34%) model. The bootstrap values were calculated using 1000 replicates. The subtree-pruning-regrafting method was chosen for the tree searching with the initial tree by NJ/BIONJ. The evolutionary distances were calculated using the program MEGA6 with the JTT (Jones et al. 1992) + gamma distribution ($\alpha = 3.63$) model. The pairwise deletion method was used for the gap treatment.

Supplementary Data

Supplementary data for this article are available online at http://glycob.oxfordjournals.org/.

Funding

This research is supported by Kagawa University Scientific Research encourages research funding 2014.

Conflict of interest statement

None declared.

Abbreviations

BS^3, bis(sulfosuccinimidyl) suberate; DLS, dynamic light scattering; LacNAc, *N*-acetyllactosamine.

References

Ahmad N, Gabius HJ, Andre S, Kaltner H, Sabesan S, Roy R, Liu B, Macaluso F, Brewer CF. 2004. Galectin-3 precipitates as a pentamer with synthetic multivalent carbohydrates and forms heterogeneous cross-linked complexes. *J Biol Chem*. 279:10841–10847.

Ahmed H, Pohl J, Fink NE, Strobel F, Vasta GR. 1996. The primary structure and carbohydrate specificity of a beta-galactosyl-binding lectin from toad (Bufo arenarum Hensel) ovary reveal closer similarities to the mammalian galectin-1 than to the galectin from the clawed frog Xenopus laevis. *J Biol Chem*. 271:33083–33094.

Ban M, Yoon HJ, Demirkan E, Utsumi S, Mikami B, Yagi F. 2005. Structural basis of a fungal galectin from Agrocybe cylindracea for recognizing sialoconjugate. *J Mol Biol*. 351:695–706.

Barondes SH, Castronovo V, Cooper DN, Cummings RD, Drickamer K, Feizi T, Gitt MA, Hirabayashi J, Hughes C, Kasai K, et al. 1994a. Galectins: A family of animal beta-galactoside-binding lectins. *Cell*. 76:597–598.

Barondes SH, Cooper DN, Gitt MA, Leffler H. 1994b. Galectins. Structure and function of a large family of animal lectins. *J Biol Chem*. 269:20807–20810.

Bourne Y, Bolgiano B, Liao DI, Strecker G, Cantau P, Herzberg O, Feizi T, Cambillau C. 1994. Crosslinking of mammalian lectin (galectin-1) by complex biantennary saccharides. *Nat Struct Biol*. 1:863–870.

Brewer CF. 2002. Binding and cross-linking properties of galectins. *Biochim Biophys Acta*. 1572:255–262.

Camby I, Le Mercier M, Lefranc F, Kiss R. 2006. Galectin-1: A small protein with major functions. *Glycobiology*. 16:137R–157R.

Cao Z, Said N, Amin S, Wu HK, Bruce A, Garate M, Hsu DK, Kuwabara I, Liu FT, Panjwani N. 2002. Galectins-3 and -7, but not galectin-1, play a role in re-epithelialization of wounds. *J Biol Chem*. 277:42299–42305.

Cardoso M, Cobacho N, Cherobim M, Pinto M, Santos C. 2014. Insights into the antimicrobial activities of unusual antimicrobial peptide families from amphibian skin. *J Clin Toxicol*. 4:205.

Collaborative Computational Project, Number 4. 1994. The CCP4 suite – Programs for protein crystallography. *Acta Crystallogr D Biol Crystallogr*. 50:760–763.

Conlon JM, Mechkarska M, Lukic ML, Flatt PR. 2014. Potential therapeutic applications of multifunctional host-defense peptides from frog skin as anti-cancer, anti-viral, immunomodulatory, and anti-diabetic agents. *Peptides*. 57C:67–77.

Cooper DN. 2002. Galectinomics: Finding themes in complexity. *Biochim Biophys Acta*. 1572:209–231.

Cooper DN, Barondes SH. 1999. God must love galectins; he made so many of them. *Glycobiology*. 9:979–984.

Copits BA, Vernon CG, Sakai R, Swanson GT. 2014. Modulation of ionotropic glutamate receptor function by vertebrate galectins. *J Physiol*. 592:2079–2096.

Diehl C, Engstrom O, Delaine T, Hakansson M, Genheden S, Modig K, Leffler H, Ryde U, Nilsson UJ, Akke M. 2010. Protein flexibility and conformational entropy in ligand design targeting the carbohydrate recognition domain of galectin-3. *J Am Chem Soc*. 132:14577–14589.

Earl LA, Bi S, Baum LG. 2011. Galectin multimerization and lattice formation are regulated by linker region structure. *Glycobiology*. 21:6–12.

Emsley P, Cowtan K. 2004. Coot: Model-building tools for molecular graphics. *Acta Crystallogr D Biol Crystallogr*. 60:2126–2132.

Ermakova E, Miller MC, Nesmelova IV, Lopez-Merino L, Berbis MA, Nesmelov Y, Tkachev YV, Lagartera L, Daragan VA, Andre S, et al. 2013. Lactose binding to human galectin-7 (p53-induced gene 1) induces long-range effects through the protein resulting in increased dimer stability and evidence for positive cooperativity. *Glycobiology*. 23:508–523.

Freymann DM, Nakamura Y, Focia PJ, Sakai R, Swanson GT. 2012. Structure of a tetrameric galectin from Cinachyrella sp. (ball sponge). *Acta Crystallogr D Biol Crystallogr*. 68:1163–1174.

Hamelryck TW, Moore JG, Chrispeels MJ, Loris R, Wyns L. 2000. The role of weak protein-protein interactions in multivalent lectin-carbohydrate binding: Crystal structure of cross-linked FRIL. *J. Mol. Biol*. 299:875–883.

Hirabayashi J, Kasai K. 1993. The family of metazoan metal-independent beta-galactoside-binding lectins: Structure, function and molecular evolution. *Glycobiology*. 3:297–304.

Houzelstein D, Goncalves IR, Fadden AJ, Sidhu SS, Cooper DN, Drickamer K, Leffler H, Poirier F. 2004. Phylogenetic analysis of the vertebrate galectin family. *Mol Biol Evol*. 21:1177–1187.

Iwaki J, Tateno H, Nishi N, Minamisawa T, Nakamura-Tsuruta S, Itakura Y, Kominami J, Urashima T, Nakamura T, Hirabayashi J. 2011. The Galbeta-(syn)-gauche configuration is required for galectin-recognition disaccharides. *Biochim Biophys Acta*. 1810:643–651.

Jones DT, Taylor WR, Thornton JM. 1992. The rapid generation of mutation data matrices from protein sequences. *Comput Appl Biosci*. 8:275–282.

Kamiya H, Muramoto K, Goto R. 1988. Purification and properties of agglutinins from conger eel, Conger Myriaster (Brevoort), skin mucus. *Dev Comp Immunol*. 12:309–318.

Krissinel E, Henrick K. 2007. Inference of macromolecular assemblies from crystalline state. *J Mol Biol*. 372:774–797.

Leonidas DD, Vatzaki EH, Vorum H, Celis JE, Madsen P, Acharya KR. 1998. Structural basis for the recognition of carbohydrates by human galectin-7. *Biochemistry (Mosc)*. 37:13930–13940.

Downloaded from https://academic.oup.com/glycob/article/25/7/792/1988836 by guest on 16 August 2022

Marschal P, Cannon V, Barondes SH, Cooper DN. 1994. Xenopus laevis L-14 lectin is expressed in a typical pattern in the adult, but is absent from embryonic tissues. *Glycobiology*. 4:297–305.

Marschal P, Herrmann J, Leffler H, Barondes SH, Cooper DN. 1992. Sequence and specificity of a soluble lactose-binding lectin from Xenopus laevis skin. *J Biol Chem*. 267:12942–12949.

Murshudov GN, Vagin AA, Dodson EJ. 1997. Refinement of macromolecular structures by the maximum-likelihood method. *Acta Crystallograph D Biol Crystallogr*. 53:240–255.

Nakamura O, Inaga Y, Suzuki S, Tsutsui S, Muramoto K, Kamiya H, Watanabe T. 2007. Possible immune functions of congerin, a mucosal galectin, in the intestinal lumen of Japanese conger eel. *Fish Shellfish Immunol*. 23:683–692.

Nesmelova IV, Ermakova E, Daragan VA, Pang M, Menendez M, Lagartera L, Solis D, Baum LG, Mayo KH. 2010. Lactose binding to galectin-1 modulates structural dynamics, increases conformational entropy, and occurs with apparent negative cooperativity. *J Mol Biol*. 397:1209–1230.

Nishi N, Abe A, Iwaki J, Yoshida H, Itoh A, Shoji H, Kamitori S, Hirabayashi J, Nakamura T. 2008. Functional and structural bases of a cysteine-less mutant as a long-lasting substitute for galectin-1. *Glycobiology*. 18:1065–1073.

Nowak TP, Haywood PL, Barondes SH. 1976. Developmentally regulated lectin in embryonic chick muscle and a myogenic cell line. *Biochem Biophys Res Commun*. 68:650–657.

Otwinowski Z, Minor W. 1997. Processing of X-ray diffraction data collected in oscillation mode. In: Carter CWJ, Sweet RM, editors. *Macromolecular Crystallography, Part A*. San Diego: Academic Press. p. 307–326.

Rabinovich GA, Toscano MA, Jackson SS, Vasta GR. 2007. Functions of cell surface galectin-glycoprotein lattices. *Curr Opin Struct Biol*. 17:513–520.

Salomonsson E, Larumbe A, Tejler J, Tullberg E, Rydberg H, Sundin A, Khabut A, Frejd T, Lobsanov YD, Rini JM, et al. 2010. Monovalent interactions of galectin-1. *Biochemistry (Mosc)*. 49:9518–9532.

Sato S, St-Pierre C, Bhaumik P, Nieminen J. 2009. Galectins in innate immunity: Dual functions of host soluble beta-galactoside-binding lectins as damage-associated molecular patterns (DAMPs) and as receptors for pathogen-associated molecular patterns (PAMPs). *Immunol Rev*. 230:172–187.

Shirai T, Mitsuyama C, Niwa Y, Matsui Y, Hotta H, Yamane T, Kamiya H, Ishii C, Ogawa T, Muramoto K. 1999. High-resolution structure of the conger eel galectin, congerin I, in lactose-liganded and ligand-free forms: Emergence of a new structure class by accelerated evolution. *Structure*. 7:1223–1233.

Shoji H, Nishi N, Hirashima M, Nakamura T. 2003. Characterization of the Xenopus galectin family. Three structurally different types as in mammals and regulated expression during embryogenesis. *J. Biol. Chem*. 278:12285–12293.

Shoji H, Nishi N, Hirashima M, Nakamura T. 2002. Purification and cDNA cloning of Xenopus liver galectins and their expression. *Glycobiology*. 12:163–172.

Tamura K, Stecher G, Peterson D, Filipski A, Kumar S. 2013. MEGA6: Molecular evolutionary genetics analysis version 6.0. *Mol Biol Evol*. 30:2725–2729.

Than NG, Romero R, Kim CJ, McGowen MR, Papp Z, Wildman DE. 2012. Galectins: Guardians of eutherian pregnancy at the maternal-fetal interface. *Trends Endocrinol Metab*. 23:23–31.

Tracey BM, Feizi T, Abbott WM, Carruthers RA, Green BN, Lawson AM. 1992. Subunit molecular mass assignment of 14,654 Da to the soluble beta-galactoside-binding lectin from bovine heart muscle and demonstration of intramolecular disulfide bonding associated with oxidative inactivation. *J Biol Chem*. 267:10342–10347.

Uchiyama H, Komazaki S, Oyama M, Matsui T, Ozeki Y. 1997. Distribution and localization of galectin purified from Rana catesbeiana oocytes. *Glycobiology*. 7:1159–1165.

Ueda T, Nakamura Y, Smith CM, Copits BA, Inoue A, Ojima T, Matsunaga S, Swanson GT, Sakai R. 2013. Isolation of novel prototype galectins from the marine ball sponge Cinachyrella sp. guided by their modulatory activity on mammalian glutamate-gated ion channels. *Glycobiology*. 23: 412–425.

Vagin A, Teplyakov A. 2000. An approach to multi-copy search in molecular replacement. *Acta Crystallograph D Biol Crystallogr*. 56:1622–1624.

Walser PJ, Haebel PW, Kunzler M, Sargent D, Kues U, Aebi M, Ban N. 2004. Structure and functional analysis of the fungal galectin CGL2. *Structure*. 12:689–702.

Whelan S, Goldman N. 2001. A general empirical model of protein evolution derived from multiple protein families using a maximum-likelihood approach. *Mol Biol Evol*. 18:691–699.

Downloaded from https://academic.oup.com/glycob/article/25/7/792/1988836 by guest on 16 August 2022